$Ni^+$ dehydrogenates propane and isobutane by an apparently exothermic 1,2 process,[25] which occurs with moderate cross section at low energy (Table I). It is not clear why the 1,2 process "turns off" with straight-chain hydrocarbons with more than three carbons. If the initial insertion into a C–H bond is reversible, then the metal ion may sample several insertion sites in a single encounter.[26] To explain the present results requires that further reaction of the C–C insertion intermediates occurs with greater facility (higher frequency factors, lower activation energies) than that of the C–H insertion intermediates. As noted in the Experimental Section, the 1,2 process is observed with *n*-butane at relative kinetic energies above ~1 eV.

(26) Multiple encounter reactions are a well-established feature of ion–molecule reactions owing to the strong ion-neutral attractive interaction. See, for example: Dugan, J. V., Jr.; Rice, J. H.; Magee, J. L. *Chem. Phys. Lett.* **1969**, *3*, 323. Sullivan, S. A.: Beauchamp, J. L. *J. Am. Chem. Soc.* **1977**, *99*, 5017.

**Acknowledgment.** This research was supported in part by the U.S. Department of Energy at Caltech and by the National Science Foundation under Grant CHE-76-17304 at MIT. Graduate fellowship support from Bell Laboratories and Sohio (L.F.H.) is gratefully acknowledged.

**Registry No.** $C_3H_8$, 74-98-6; *n*-$C_4H_{10}$, 106-97-8; *i*-$C_4H_{10}$, 75-28-5; *n*-$C_5H_{12}$, 109-66-0; *neo*-$C_5H_{12}$, 463-82-1; *n*-$C_6H_{14}$, 110-54-3; $Ni^+$, 14903-34-5; butane-*1,1,1,4,4,4-d*$_6$, 13183-67-0; pentane-*1,1,1,5,5,5-d*$_6$, 32740-32-2; pentane-*2,2,3,3,4,4-d*$_6$, 81194-30-1; hexane-*1,1,1,6,6,6-d*$_6$, 32740-20-8; hexane-*2,2,5,5-d*$_4$, 32740-23-1; hexane-*3,3,4,4-d*$_4$, 32740-24-2; hexane-*1,1,6,6-d*$_4$, 83174-87-2; hexane-*3,3-d*$_2$, 32740-25-3; cyclopentanone, 120-92-3.

# Peptide Conformation. 17.[1] *cyclo*-(L-Pro-L-Pro-D-Pro). Conformational Analysis by 270- and 500-MHz One- and Two-Dimensional $^1H$ NMR Spectroscopy

**Horst Kessler,* Wolfgang Bermel, Axel Friedrich, Gerhard Krack, and William E. Hull**

*Contribution from the Institut für Organische Chemie, der Universität Frankfurt, Niederurseler Hang, D-6000 Frankfurt 50, Federal Republic of Germany, and Bruker Analytische Messtechnik GmbH, Silberstreifen, D-7512 Rheinstetten-Fo, Federal Republic of Germany.* *Received February 16, 1982*

**Abstract:** The 270- and 500-MHz $^1H$ NMR spectra of *cyclo*-(L-Pro$_2$-D-Pro) in various solvents have been analyzed with the aid of one- and two-dimensional (2-D) NMR techniques; 500-MHz 2-D-*J*-resolved spectra were used to determine starting parameters for chemical shift values and to assign overlapping spin multiplets of the individual nuclei in the 21-spin system. 2-D spin-echo-correlated spectra yield connectivities between coupled spins. In particular, many small long-range couplings have been detected by this technique. Stereochemical assignment of geminal proline protons has been performed by 2-D nuclear Overhauser enhancement (2-D NOE) spectroscopy and by interpretation of aromatic solvent-induced shift (ASIS) effects, coupling constants, and carbonyl anisotropy. A twisted-boat backbone conformation similar to the structure determined by X-ray analysis was derived from the data.

## Introduction

In an earlier report we described the $^1H$ NMR study of *cyclo*-(L-Pro$_3$), which has an effective $C_3$ symmetry in solution and could be analyzed as a seven-spin system.[2] The subject of this paper is *cyclo*-(L-Pro-L-Pro-D-Pro) (**1**), which presents a much more complicated spectrum.[3] To a first approximation it can be considered to be the sum of three separate seven-spin systems, corresponding to the three nonequivalent proline units. However, resolution-enhanced $^1H$ spectra demonstrate that measurable interresidual long-range $^5J$ couplings exist across the amide bonds. Thus, in the final analysis **1** must be handled as a 21-spin system.

The rather difficult analysis of this system is of interest since **1** is an example of a cyclotripeptide containing residues of differing chirality and can, therefore, exist only in the boat backbone conformation.[4-6] In addition, the $^1H$ NMR data should allow a determination of the proline ring conformations in solution, enabling a comparison with X-ray structure data[3,7] and solid-state NMR results for the crystal.[1]

## Results and Discussion

The 270-MHz $^1H$ NMR spectrum of **1** in $CDCl_3$ shows considerable overlapping in the $\beta$- and $\gamma$-proton region between 1.5 and 2.3 ppm from $Me_4Si$ (Figure 1). A significant improvement in spectral dispersion is seen at 500 MHz and in $CD_2Cl_2$ solution, so that an analysis can be attempted. The addition of deuteriobenzene to a $CDCl_3$ solution of **1** produces remarkable changes in the spectrum and simplifies the analysis for several groups. The NMR parameters that were obtained for samples containing different solvents or solvent mixtures have been compared and checked for consistency (see below).

**Assignment of the $^1H$ Signals to Seven Spin Systems.** For the first stage of the spin-system analysis, the long-range interresidue *J* couplings were ignored. Thus, we are dealing with three overlapping seven spin systems. The signals of the $\alpha$ protons (>4 ppm) and the $\delta$ protons (3–4 ppm) can be identified immediately. However, the $\beta$ and $\gamma$ signals can be assigned only by double-resonance or two-dimensional NMR techniques. In these cases

* Address correspondence to this author at the Institut für Organische Chemie der Universität Frankfurt.

(1) Peptide Conformation. 16: Kessler, H.; Bermel, W.; Förster, H. *Angew. Chem.* **1982**, *94*, 703; *Angew. Chem., Int. Ed. Engl.* **1982**, *21*, 689.
(2) Kessler, H.; Friedrich, A.; Hull, W. E. *J. Org. Chem.* **1981**, *46*, 3892.
(3) Bats, J. W.; Friedrich, A.; Fuess, H.; Kessler, H.; Mästle, W.; Rothe, M. *Angew. Chem.* **1979**, *91*, 573; *Angew. Chem., Int. Ed. Engl.* **1979**, *18*, 538.
(4) Kessler, H.; Kondor, P.; Krack, G.; Krämer, P. *J. Am. Chem. Soc.* **1978**, *100*, 2548.
(5) Kessler, H. In "Stereodynamics of Molecular Systems"; Sarma, H., Ed. Pergamon Press: New York, 1979; p 187.
(6) Kessler, H.; Krämer, P.; Krack, G. *Isr. J. Chem.* **1980**, *20*, 188.
(7) Bats, J. W., Fuess, H. *J. Am. Chem. Soc.* **1980**, *102*, 2065.

0002-7863/82/1504-6297$01.25/0 

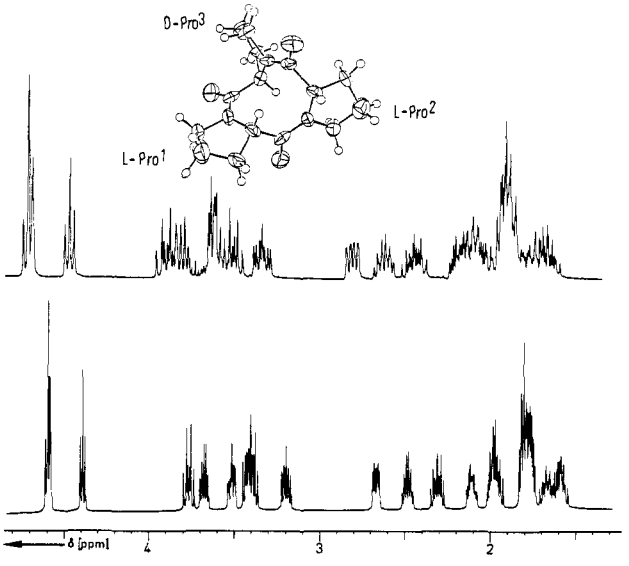


**Figure 1.** X-ray structure and $^1$H NMR spectra of *cyclo*-(L-Pro$_2$-D-Pro) at 270 MHz in $CDCl_3$ (above) and at 500 MHz in $CD_2Cl_2$ (below).

of strong signal overlap, decoupling difference spectra and, even more important, double-INDOR difference spectroscopy[8] proved quite useful. The latter is extremely selective since only two individual transitions of a given spin multiplet are perturbed and difference spectra are generated. With this technique the three seven-spin systems were localized,[8] and the results were later confirmed by two-dimensional NMR techniques.

**Assignment of Each Seven-Spin System to Its Corresponding Proline Residue.** After the individual seven-spin systems had been identified, it was necessary to make assignments to specific proline residues in the sequence. As a starting point $^{13}$C NMR spectroscopy was used.[5] From topochemical arguments[5,6] it follows that in the boat conformation of *cyclo*-(L-Pro$_2$-*N*-BzlGly) the achiral residue *N*-benzylglycine (*N*-BzlGly) can take only the position of the D-Pro in **1**. In the $^{13}$C NMR spectrum of this analogue as well as that of *cyclo*-(L-Pro$_2$-Sar), the set of signals corresponding to Pro$^3$ are replaced by those of the nonproline residue.[5,6,9,10] L-Pro$^2$ could be recognized by the downfield shifts for $C_\alpha$ and $C_\beta$, characteristic of the unusual $\Psi_2$ angle of −20° for the boat conformation,[4] Proton–carbon connectivities were elucidated by selective proton decoupling experiments.[9,31] To support these previously obtained assignments the $^1$H NMR spectra of a complete series of peptides *cyclo*-(L,D-Pro$_n$-*N*-BzlGly$_{3-n}$), $n$ = 0–3, were investigated independently.[6] The solvent-induced shifts caused by benzene (ASIS) or $Me_2SO$ led to a convincing assignment of the resonances from D-Pro.[3,6] For the final chemical proof the analogue *cyclo*-(L-Pro-L-Pro-D-($\alpha$-$^2$H)Pro) (**1d**) was synthesized. The $^1$H NMR spectrum of **1d** in $CDCl_3/C_6D_6$ shows that the doublet at 4.5 ppm (Figure 5) is missing.

Hence, three independent methods have been used to securely assign the D-Pro$^3$ spin system. The distinguishing of the two L-Pro systems rested at first solely on $^{13}$C chemical shift data.[4,9] In the detailed analysis of the 500-MHz $^1$H spectra the significance of the interresidue $^5J$ couplings[11] was recognized, and through low-power selective decoupling experiments the $^5J$ couplings were used to achieve an independent sequence assignment of the three proline spin systems, confirming the conclusions reached previously. The long-range interactions could also be observed in a more elegant way via the two-dimensional scalar-correlated $^1$H NMR experiment (SECSY).[12]

The most compact representation of the 2-D data matrix is the contour plot, which presents peak intensity contours in a rectangular plot with $x$, $y$ axes given by the frequencies $\omega_2$ and $\omega_1$, respectively. The $\omega_2$ axis represents the $^1$H chemical shifts, and the $\omega_1$ axis represents the correlation frequency axis (Figure 2). The horizontal axis ($\omega_1 = 0$) contains essentially the normal 1-D spectrum with the various multiplets appearing at their normal chemical shift positions ($\omega_2$). If two spins A and B share a scalar $J$ coupling, then a pair of off-axis multiplet signals appears with coordinates $(\omega_A, (\omega_A - \omega_B)/2)$ and $(\omega_B, (\omega_B - \omega_A)/2)$. Thus, coupling constant information has been transformed into information about differences in chemical shifts. It is, therefore, possible to observe correlation peaks even when couplings are very small (in this case less than 0.4 Hz) and not resolved. For small couplings the correlation peak intensity is roughly proportional to the magnitude of the coupling constant. Given sufficient signal-to-noise in the 2-D spectrum, it is then possible to not only detect these long-range effects but also to estimate the magnitude of the coupling for use in spectra simulations.

As can be seen from the expressions for the coordinates of the off-axis correlation peaks, a straight line joining the positive and negative (relative to $\omega_1 = 0$) peaks has a slope of unity and crosses the horizontal axis midway between the two chemical shifts (Figure 3a). This has been the usual technique for analyzing the correlations and determining the chemical shifts of spins which are coupled. A simpler and easier to visualize method involves constructing parallel lines with slope $^1/_2$ and passing through each of the known chemical shift positions. All correlation peaks involving a particular spin will then lie on the line passing through its chemical shift ($\omega_2$) at $\omega_1 = 0$ (Figure 3b). The chemical shifts of those spins that are coupled to a chosen spin are immediately recognized as the $x$ coordinates of the correlation peaks. Figure 2 demonstrates this technique for the cyclic peptide **1**. An expanded region of the SECSY spectrum is given in Figure 4 and shows clearly the long-range interresidue $^5J$-coupling correlations which provided a sequence assignment of the three proline spin systems.

The $\alpha$ proton of Pro$^3$ is found to couple with the $\alpha$ proton and low-field $\alpha$ proton ($\delta_1^t$) of Pro$^1$. In fact, a weak correlation is also found for $\alpha_3$ with $\delta_1^c$. Such interresidue couplings from protons can come only from the proline *following* in the sequence, i.e., Pro$^3$-Pro$^1$. The $\alpha$ proton of Pro$^2$ ($\alpha_2$) shows coupling to the two $\delta$ protons of Pro$^3$, which follows in the sequence Pro$^2$-Pro$^3$-Pro$^1$; thus, the assignments are complete. Interestingly, a sizable coupling between two $\alpha$ protons is observed only for the pair $\alpha_1\alpha_3$. The sequence analysis made here via scalar coupling is confirmed by an analysis of dipolar interactions (NOE) to be discussed below.

**Analysis of the Proline Spin Systems.** The 500-MHz two-dimensional $J$-resolved $^1$H NMR spectra[13] proved to be quite valuable for a detailed spin system analysis. The data matrix was processed in the conventional way with 45° tilt and projection to give a proton chemical shift spectrum. This is illustrated in Figure 5 for a sample dissolved in $C_6D_6/CDCl_3$. It is important to note that two extra signals appear, one midway between the two Pro$^1$ $\delta$ protons at 3.547 ppm and the other midway between the Pro$^2$ $\gamma$ protons at 1.128 ppm. This is a result of the second-order character of these two spin systems (AB effect). In practice such additional peaks will often occur in complicated spin systems, even at very high magnetic field strengths.

Correlations between coupled spins were determined from the SECSY spectrum as described above. Geminal and vicinal couplings were indicated by strong correlation peaks, and the magnitude of these couplings could be estimated by examining cross sections through the 2-D $J$-resolved data matrix. One particular advantage of the SECSY spectrum is evident in Figure 2. For example, the $\alpha$ proton of Pro$^3$ appears as a broad doublet with a vicinal coupling to $\beta_3^c$ and no less than six long-range couplings of less than 1 Hz. These cannot be resolved in a one-

(8) Kessler, H., Krack, G., Zimmermann, G. *J. Magn. Reson.* **1981**, *44*, 208.
(9) Friedrich, A., Thesis, Frankfurt, 1980.
(10) Krack, G., Thesis, Frankfurt, 1981.
(11) Davies, D. B.; Abu Khaled, M.; Urry, D. W. *J. Chem. Soc.*, Perkin *Trans. 2* **1977**, 1294.
(12) Nagayama, K.; Wüthrich, K.; Ernst, R. R. *Biochem. Biophys. Res. Commun.* **1979**, *90*, 305. Nagayama, K.; Kumar, A.; Wüthrich, K.; Ernst, R. R. *J. Magn. Reson.* **1980**, *40*, 321.
(13) Aue, W. P.; Bartholdi, E.; Ernst, R. R. *J. Chem. Phys.* **1976**, *64*, 2229. Nagayama, K.; Bachmann, P.; Wüthrich, K.; Ernst, R. R. *J. Magn. Reson.* **1978**, *31*, 133.

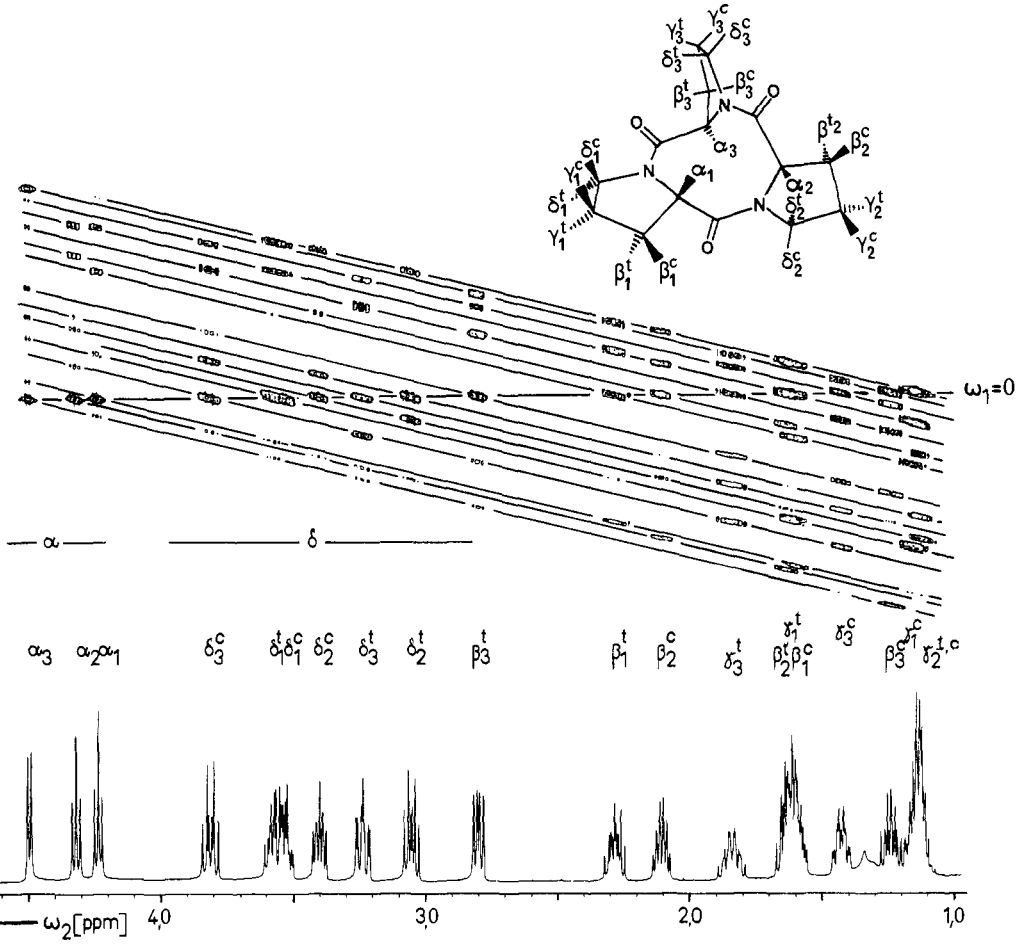


**Figure 2.** 500-MHz 2-D spin-echo-correlated $^1H$ NMR spectrum (SECSY) of *cyclo*-(L-$Pro_2$-D-Pro) in $CDCl_3/C_6D_6$ (1:8).

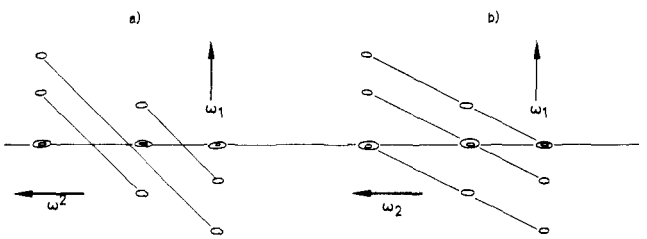


**Figure 3.** Evaluation of the SECSY spectrum. The conventional method is represented in the left part (a). Evaluation via (b) is preferred (see text).

dimensional spectrum even with resolution enhancement. The use of one-dimensional selective decoupling techniques to analyze the multitude of long-range couplings in **1** would be extremely tedious.

For spectral simulations the three seven-spin systems were considered separately, and first estimates for the coupling constants were taken from the *J*-resolved cross sections. The program PANIC[14] was used to first visually compare observed and calculated spectra. After considerable manipulation of parameters to obtain a reasonable match, as many lines were assigned as possible and a least-squares iteration performed. The chemical shift dispersion of the individual spin systems varied considerably with changes in solvent. Therefore, the 500-MHz $^1H$ spectra in $CD_2Cl_2$ and in $CDCl_3/C_6D_6$ were both analyzed. In $CD_2Cl_2$ one finds that the $Pro^1$ system is particularly well dispersed. On the other hand, $Pro^3$ was most readily solved with the $C_6D_6$ solvent mixture. Unfortunately, $Pro^2$ is not well dispersed in any solvent, an iterative fit was not possible for the complete seven-spin systems, and the error limits for the spectral parameters are correspondingly larger. Since the precision of the iterative analysis varied with choice of solvent, it was not possible to recognize any distinct solvent dependence of the coupling constants; i.e., vicinal couplings varied by less than 0.3 Hz. Thus, coupling parameters determined by iterative fitting of the spectrum in $CD_2Cl_2$ were combined with chemical shifts determined from the 2-D-*J*-resolved spectrum in $CDCl_3/C_6D_6$ to produce the calculated spectrum shown in Figure 6.

The problems involved in this analysis are readily seen by examining expanded portions of the experimental and calculated spectra in the $\beta$- and $\gamma$-proton region (Figure 7). At the most upfield position three-proton multiplets overlap, and the two $\gamma_2$ protons are a strongly coupled AB system. Thus, an adequate assignment of transitions could not be realized prior to iteration, and the agreement between calculated and observed spectra is poorer than that obtained for other regions in the spectrum. Very small changes in chemical shifts or couplings produce large changes in the calculated spectrum for the overlapping $\gamma$ protons. Excellent simulations could be obtained for the other multiplets, in particular, the $\alpha$ and $\beta$ regions which are not shown. The chemical shifts and coupling constants are summarized in Tables I and II.

Since direct analysis of the complete 21-spin system with inter-residue long-range couplings was not feasible, the following method was used to remove interresidue couplings. Using the sample of **1** in $CDCl_3/C_6D_6$ at 500 MHz, three decoupling experiments were performed with irradiation of each $\alpha$ proton using the minimum power necessary to remove long-range couplings. By combining appropriate regions from the original spectrum and these decoupled spectra, it was possible to create three "synthetic" spectra, one for each proline, in which isolated seven-spin systems could be studied. The interresidue $^5J$ couplings are summarized in Table III.

During manipulation of the calculated spectra it was observed that in most cases the relative signs of the long-range couplings had little influence on the results. Therefore, only positive signs were used. To our knowledge only one of the previous studies

(14) PANIC, program for iterative spin simulation, Bruker NMR software.

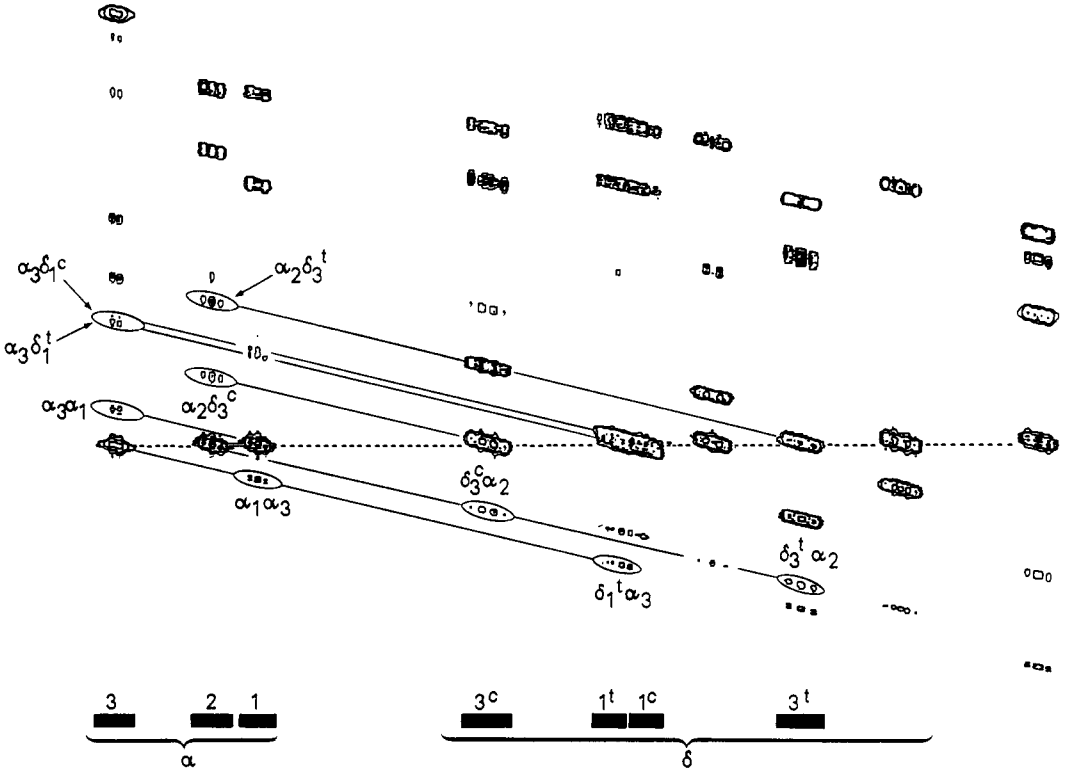


**Figure 4.** Part of the 500-MHz SECSY spectrum of *cyclo*-(L-Pro$_2$-D-Pro). Correlation peaks caused by coupling across the amide bonds are encircled and correlation lines as shown in Figure 3b are drawn.

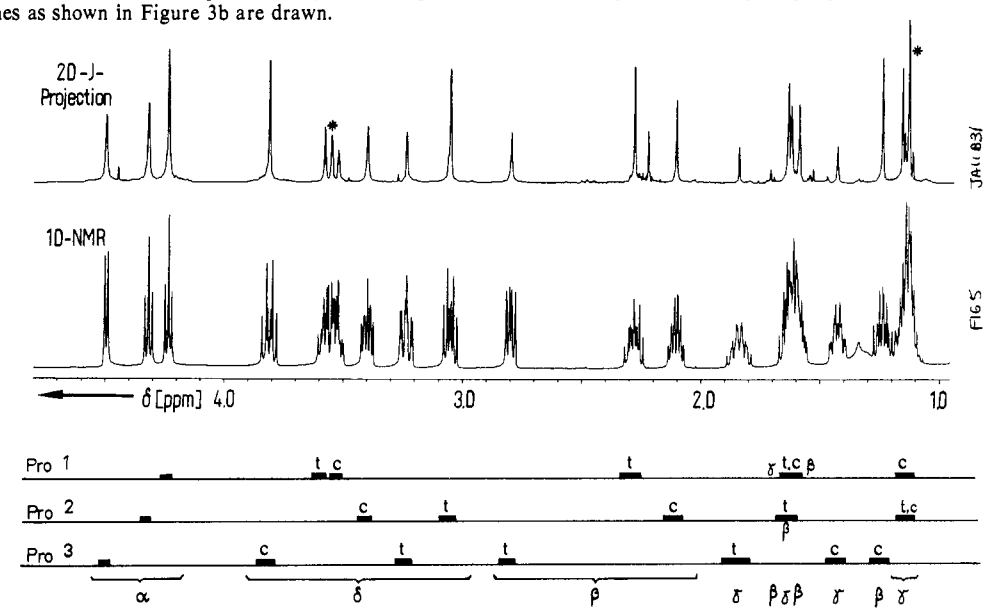


**Figure 5.** One-dimensional $^1$H NMR spectrum and projection of the 500-MHz 2-D-*J*-resolved spectrum of *cyclo*-(L-Pro$_2$-D-Pro) in $CDCl_3/C_6D_6$ (1:8). The peaks marked (*) arise from strong AB effects. Assignments of the proline protons are given below (c = cis to α-H, t = trans to α-H).

Table I. Proton Chemical Shifts of *cyclo*-(L-Pro$^1$-L-Pro$^2$-D-Pro$^3$) in $CD_2Cl_2$ and $CDCl_3/C_6D_6$ (1:8)

| | Pro$^1$ | | | Pro$^2$ | | | Pro$^3$ | | |
|---|---|---|---|---|---|---|---|---|---|
| | $CD_2Cl_2$[a] (ppm) | $CDCl_3/C_6D_6$ (1:8)[a] (ppm) | ASIS[b] (Hz at 270 MHz) | $CD_2Cl_2$[a] (ppm) | $CDCl_3/C_6D_6$ (1:8)[a] (ppm) | ASIS[b] (Hz at 270 MHz) | $CD_2Cl_2$[a] (ppm) | $CDCl_3/C_6D_6$ (1:8)[a] (ppm) | ASIS[b] (Hz at 270 MHz) |
| α | 4.385 | 4.230 | −58 | 4.589 | 4.315 | −104 | 4.586 | 4.493 | −47 |
| $\beta^c$ | 2.098 | 1.576 | −160 | 2.473 | 2.095 | −149 | 1.578 | 1.226 | −127 |
| $\beta^t$ | 2.302 | 2.272 | −57 | 1.952 | 1.622 | −124 | 2.659 | 2.790 | +16 |
| $\gamma^c$ | 1.655 | 1.141 | −191 | 1.796 | 1.102 | −238 | 1.759 | 1.414 | −127 |
| $\gamma^t$ | 1.977 | 1.608 | −160 | 1.793 | 1.136 | −232 | 1.772 | 1.831 | −20 |
| $\delta^c$ | 3.506 | 3.519 | −3 | 3.671 | 3.391 | −122 | 3.761 | 3.805 | −12 |
| $\delta^t$ | 3.414 | 3.570 | −10 | 3.384 | 3.043 | −131 | 3.191 | 3.230 | −13 |

[a] Best values obtained by iterative calculation of the 500-MHz $^1$H NMR spectra (error limits ±0.001 ppm). [b] Determined from the 270-MHz $^1$H NMR spectrum in pure $CDCl_3$ and pure $C_6D_6$.

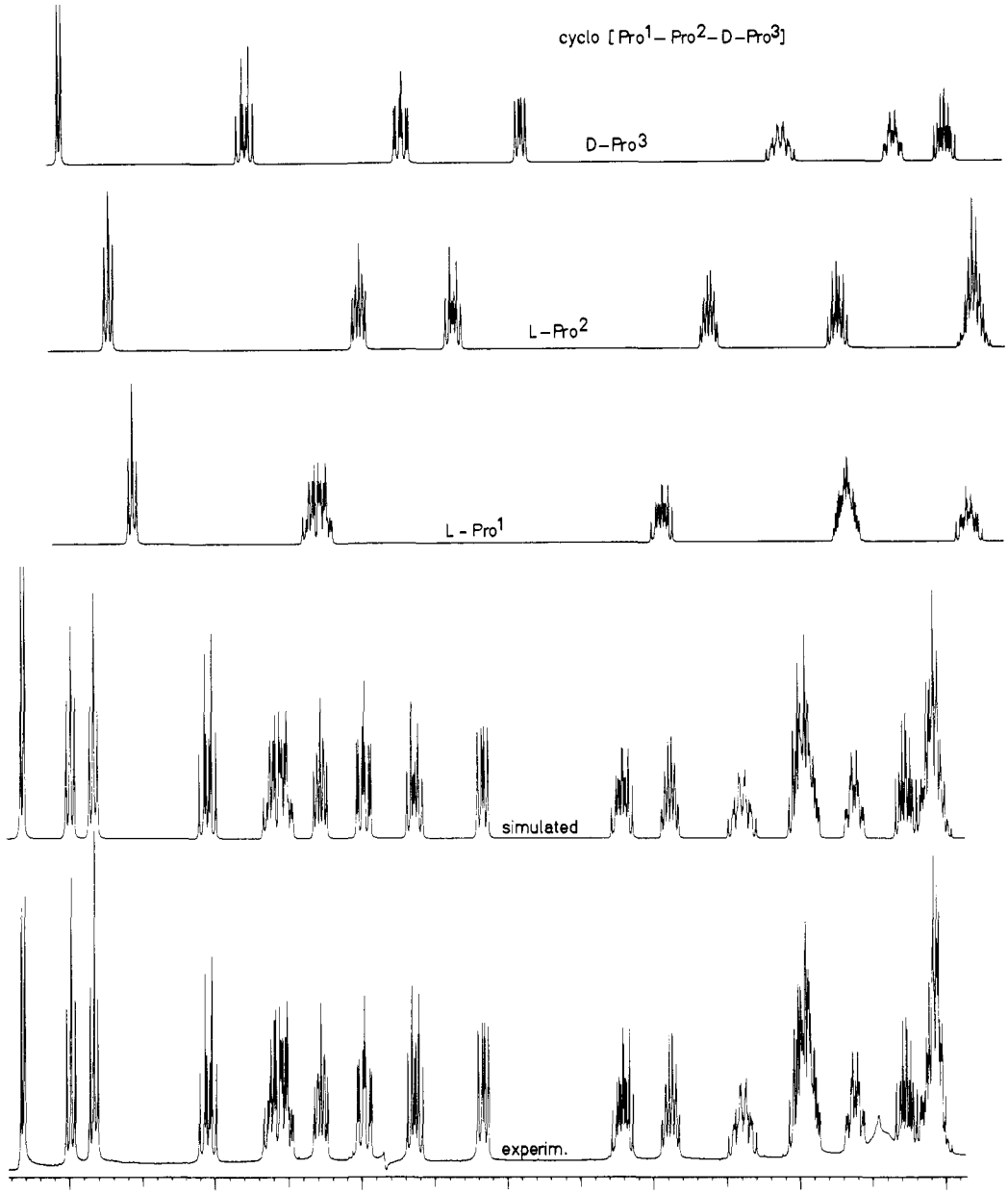


**Figure 6.** Spin simulation of the 500-MHz $^1H$ NMR spectrum of *cyclo*-(L-$Pro_2$-D-Pro) in $CDCl_3/C_6D_6$ (1:8). The three separately simulated seven-spin systems are shown above. Summation of these three spectra yield the fourth spectrum from above. The experimental spectrum is shown below.

of the proline spin system includes long-range couplings to a larger extend.[2] One long-range coupling between a $\beta$ and a $\delta$ proton in L-Pro and L-Pro-$NH_2$ has also been observed.[15]

**Assignment of Geminal Protons within Each Proline System.** One of the more difficult problems in analyzing proline spin systems is the assignment of cis- and trans-standing (relative to the $\alpha$ proton) geminal protons at each of the $\beta$, $\gamma$, $\delta$ sites. In the past this has led to errors in the assignment of the much simpler seven-spin system of *cyclo*-(L-$Pro_3$).[2,16,17] The assignments presented here are based on the following independent methods: 2-D NOE measurements, analysis of vicinal couplings, solvent effects (ASIS and $Me_2SO$-induced shifts), and consideration of the anisotropy of the neighboring amide group.

For **1** in low-viscosity solvents the homonuclear intramolecular NOE has been found to be weak and positive at 500 MHz. The magnitude of the NOE is strongly dependent upon interproton distance[18] and is, therefore, quite useful in a qualitative sense for making assignments and conformational analysis. For example, a one-dimensional NOE-difference experiment[19] at 270 MHz, where the NOE is larger positive in a molecule of this size, shows that irradiation of $\alpha_2$ produces a relative strong NOE at $\alpha_1$. This confirms the close proximity of these two protons as predicted by the X-ray structure and Dreiding models and confirms the sequence assignment given above. A large number of NOEs can be observed via the 2-D NOE technique (NOESY)[13,20] as shown in Figure 8. It is important to realize that in a many-spin system NOE magnitudes for a given pair of spins need not be the same in both directions. Thus, the correlation peaks above and below the $\omega_1 = 0$ axis are generally not of the same magnitude. As expected, the dipolar interaction and, hence, NOE for geminal

(15) Pogliani, L.; Ellenberger, M.; Valat, J.; Bellocq, A. M. *Int. J. Pept. Protein Res.*, **1975**, *7* 345. Pogliani, L.; Ellenberger, M.; Valat, J. *Org. Magn. Reson.* **1975**, *7*, 61, and references cited therein.

(16) Deber, C. M.; Torchia, D. A.; Blout, E. R. *J. Am. Chem. Soc.* **1971**, *93*, 4893.

(17) Anteunis, M. J.; Callens, R.; Asher, V.; Sleeckx, J. *Bull. Soc. Chim. Belg.* **1979**, *87*, 41.

(18) Noggle, J. H.; Schirmer, R. E. "The Nuclear Overhauser Effect"; Academic Press: New York, 1971.

(19) Gibbons, W. A.; Crepaux, D.; Delayre, J.; Dunand, J. J.; Hajdukovic, G.; Wyssbrod, H. R., "Peptides 1975"; Walter, R., Meienhofer, J., Eds.; Ann Arbor Science Publishers: Ann Arbor, Mich., 1975; p 127.

(20) Macura, S.; Huang, Y.; Suter, D.; Ernst, R. R. *J. Magn. Reson.* **1981**, *43*, 259, and references cited therein.

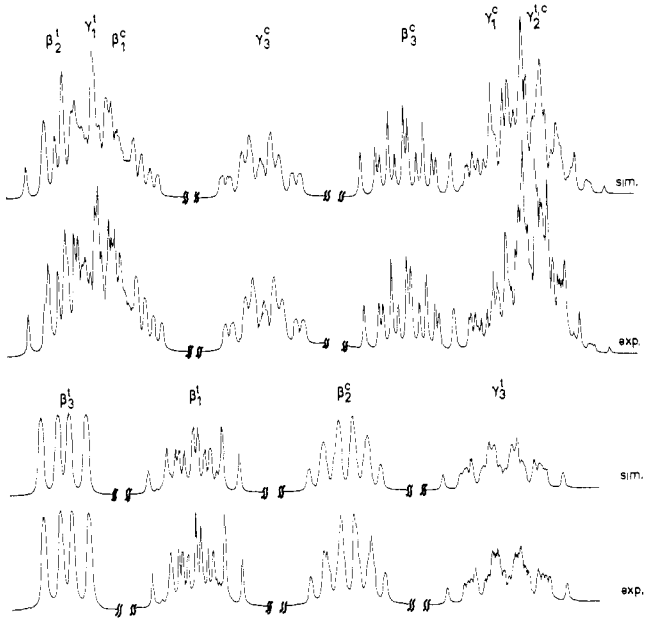


**Figure 7.** Simulated (above) and experimental (below) expansions of multiplets of the $\beta$- and $\gamma$-proton signals of *cyclo*-(L-Pro$_2$-D-Pro).

Table II. $^1$H NMR Coupling Constants for *cyclo*-(L-Pro$^1$-L-Pro$^2$-D-Pro$^3$)[a]

| | Pro$^1$ | Pro$^2$ | Pro$^3$ |
|---|---|---|---|
| $^3J\alpha\beta^c$ | 7.07 | 6.99 | 6.51 |
| $^3J\alpha\beta^t$ | 7.59 | 8.22 | 0.58 |
| $^4\alpha\gamma^c$ | <0.01 | <0.01 | 0.50 |
| $^4J\alpha\gamma^t$ | 0.58 | 0.60 | 0.62 |
| $^5J\alpha\delta^c$ | 0.59 | 0.60 | 0.01 |
| $^5J\alpha\delta^t$ | 0.59 | 0.62 | 0.44 |
| $^2J\beta^c\beta^t$ | −12.46 | −12.80 | −11.96 |
| $^3J\beta^c\gamma^c$ | 7.00 | 5.92 | 8.29 |
| $^3J\beta^c\gamma^t$ | 3.40 | 4.90 | 11.94 |
| $^4J\beta^c\delta^c$ | 0.97 | 0.52 | <0.01 |
| $^4J\beta^c\delta^t$ | 0.50 | 0.97 | 0.17 |
| $^3J\beta^t\gamma^c$ | 10.78 | 8.29 | 1.25 |
| $^3J\beta^t\gamma^t$ | 7.09 | 7.15 | 7.31 |
| $^4J\beta^t\delta^c$ | 0.45 | 0.54 | 0.39 |
| $^4J\beta^t\delta^t$ | <0.01 | 0.38 | <0.01 |
| $^2J\gamma^c\gamma^t$ | −12.30 | −12.81 | −12.68 |
| $^3J\gamma^c\delta^c$ | 7.78 | 6.88 | 9.11 |
| $^3J\gamma^c\delta^t$ | 9.89 | 7.61 | 3.30 |
| $^3J\gamma^t\delta^c$ | 3.07 | 4.90 | 8.98 |
| $^3J\gamma^t\delta^t$ | 6.69 | 8.04 | 10.23 |
| $^2J\delta^c\delta^t$ | −11.67 | −12.39 | −12.77 |
| RMS[b] | 0.06 | | 0.17 |

[a] Best values obtained by iterative calculation of the 500-MHz $^1$H NMR spectra in $CD_2Cl_2$ and $CDCl_3/C_6D_6$ (1:8). [b] RMS deviation after least-squares iteration.

Table III. $^5J$ Coupling Constants (in Hz) across the Amide Bonds Obtained by Decoupling Experiments

| $\alpha_1$ | $\alpha_2$ | $\alpha_3$ |
|---|---|---|
| $\alpha_1\alpha_2 \lesssim 0.3$ | $\alpha_2\alpha_1 \lesssim 0.3$ | $\alpha_3\alpha_2 < 0.2$ |
| $\alpha_1\alpha_3$ 0.5 | $\alpha_2\alpha_3 < 0.2$ | $\alpha_3\alpha_1$ 0.5 |
| $\alpha_1\delta_2{}^c < 0.1$ | $\alpha_2\delta_3{}^c$ 0.3 | $\alpha_3\delta_1{}^c$ 0.5 |
| $\alpha_1\delta_2{}^t < 0.1$ | $\alpha_2\delta_3{}^t$ 0.4 | $\alpha_3\delta_1{}^t$ 0.5 |

protons are particularly large. However, for assignment purposes the NOE between vicinal protons is of most importance. The effect is always larger for protons which are cis to each other than for the trans orientation.

In Figure 8 important correlation peaks have been circled and connecting lines have been drawn in a manner similar to Figure 4. For example, the $\alpha_1$ proton of Pro$^1$ shows NOE only to the upfield $\beta$ proton which must be in cis geometry ($\beta_1{}^c$). The $\alpha_2$ proton shows a larger NOE to the low-field $\beta$ proton which can be assigned $\beta_2{}^c$. For Pro$^3$ the NOE cross peak $\alpha_3\beta_3{}^c$ is only slightly larger than $\alpha_3\beta_3{}^t$, and this agrees well with the $\theta$ values determined from vicinal couplings (see below). A transannular NOE was observed between $\alpha_3$ and the high-field $\delta_2$, which from model considerations can be assigned to $\delta_2{}^t$. This is particularly useful since the stereochemical assignments for Pro$^2$ are hampered by the strong overlap in the $\gamma$ region. Finally, the NOE $\gamma_3{}^c\delta_3{}^c$ confirmed the assignment of these two protons.

The changes in chemical shifts (ASIS) introduced by adding $C_6D_6$ to a $CDCl_3$ solution of **1** are summarized in Table I. The ASIS values for Pro$^2$ are nearly the same for cis- and trans-standing protons and provide no assistance for the assignments. The discussion of the ASIS values for Pro$^1$ and Pro$^3$ is analogous to the one presented for *cyclo*-(L-Pro$_2$)[2,21] and supports the assignments given in Table I.

The anisotropy effect of the neighboring carbonyl group and shift changes induced by $Me_2SO$ could be rationalized by consideration of a Dreiding model as discussed in ref 2 and proved useful in supporting assignments.[9,10] Of course, the vicinal couplings provide very useful information for stereochemical assignments. Thus, trans-oriented protons will have the smallest vicinal couplings ($\theta$ values near 90°),[2] and this has been taken into account in Table II.

**Backbone Conformation.** The differing chiralities of the proline residues in **1** allow only the boat conformation.[3-6] This leads to a strong steric interaction between $\alpha_1$ and $\alpha_2$ (large NOE as mentioned above), which can be relieved by a twist.[5] The $\alpha_1$ proton is, thus, displaced in the direction over the amide bond Pro$^2$–Pro$^3$, and this causes a change in the $\Psi_2$ angle for the carbonyl and $C_\alpha$ in Pro$^2$. A twisting of the backbone is readily apparent in the $^1$H NMR spectrum by consideration of the $\beta$-proton chemical shifts. In a normal boat conformation the $\beta_2{}^t$ is shifted downfield relative to $\beta_2{}^c$ by the anisotropy of the Pro$^2$ carbonyl. In a twisted boat the $\beta_2{}^c$ is shifted downfield. The $\beta$-proton chemical shifts for **1** are presented in Figure 9.

One finds that for Pro$^1$ and Pro$^3$ the $\beta^t$ appears at low field, while for Pro$^2$ the $\beta_2{}^c$ is at low field. This effect of the twist is also observed in the vicinal coupling $\alpha_2\beta_2{}^t$ ($^3J$ = 8.2 Hz), which is much larger than it would be in the normal boat conformation where the $\theta$ value is nearly 90°. In the solid state the twist conformation has been demonstrated by the X-ray structure.

**Conformation of the Proline Ring.** The conformation of the proline ring has been treated in several publications.[2,15-17,22-25] The heterocyclic 5-ring has more flexibility than a 6-ring, so that the conformation is critically dependent upon the surrounding environment. The constitution of the peptide as well as crystal and solvent effects will be important. In the crystalline form of **1** the unit cell contains two molecules with different conformations.[3,7] The X-ray results have been recently confirmed by solid-state $^{13}$C NMR (CP-MAS) whereby two sets of carbon signals are observed.[1]

In general, the proline ring conformation can only be determined by an analysis of the vicinal coupling constants. Three $\chi$ angles are obtained: $\chi_1(\alpha,\beta)$, $\chi_2(\beta,\gamma)$, $\chi_3(\gamma,\delta)$. The vicinal couplings are quite dependent upon the substitution pattern and conformation of the ethane fragment. Therefore, a discussion of the $\chi$ angles neglecting these effects yields only a first approximation of the ring geometry. A simple use of the Kopple equation[24] for the various coupling constants along the same bond results in different $\chi$ angles.[26] This indicates that the proline rings are not

(21) Compare also: Kopple, K. D.; Wiley, G. R.; Tauke, R. *Biopolymers* **1973**, *12*, 627.

(22) Haasnoot, C. A. G.; De Leeuw, F. A. A. M.; De Leeuw, H. P. M.; Altona, C. *Biopolymers* **1981**, *20*, 1211, and references cited therein.

(23) Balasubramanian, R.; Lakshminarayanan, A. V.; Sabesan, M. N.; Tegoni, G.; Venkatesan, K.; Ramachandran, G. N. *Int. J. Pept. Protein Res.* **1971**, *3*, 25.

(24) (a) Bach, A. C.; Bothner-By, A. A.; Gierasch, L. M. "Peptides, Synthesis-Structure-Function" (Proceedings of the 7th American Peptide Symposium); Rich, D. H., Gross, E., Eds.; Pierce Chemical Co., Rockford, Ill., 1981; p 343; (b) *J. Am. Chem. Soc.* **1982**, *104*, 572.

(25) Bystrov, V. F. *Prog. NMR Spectrosc.* **1976**, *10*, 41, and references cited therein.

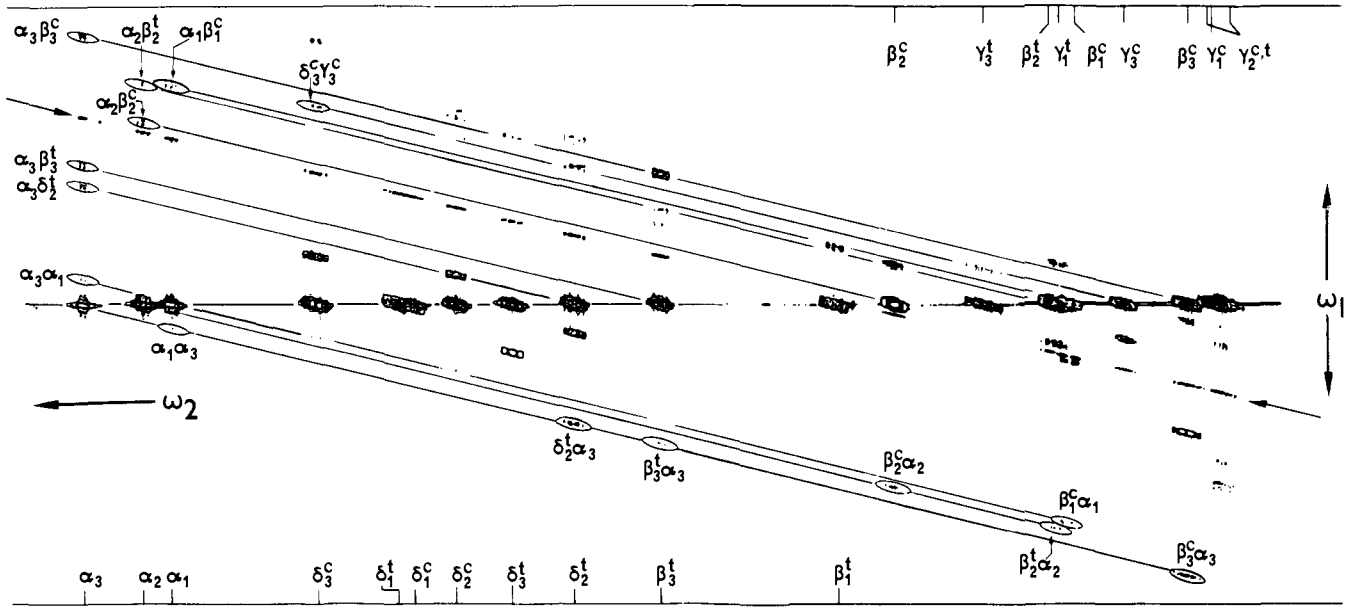

Figure 8. 500-MHz 2-D NOE spectrum of *cyclo*-(L-$Pro_2$-D-Pro). NOE effects which are discussed in the text are encircled and correlation lines are drawn corresponding to Figure 3b. The peaks on the straight line (indicated by arrows) which intersects the $\omega_1 = 0$ axis at about 2.2 ppm result from incomplete phase cycling for the three-pulse experiment (see Experimental Section).

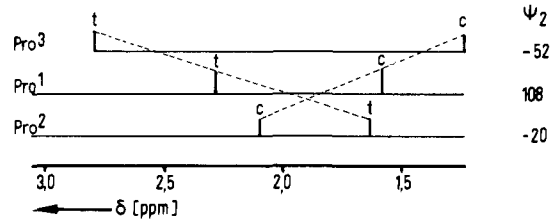

Figure 9. Chemical shift of the $\beta$ protons in *cyclo*-(L-$Pro_2$-D-Pro) and corresponding $\Psi_2$ angles.

conformationally homogeneous. Certainly also the picture of two Ramachandran envelope conformations (exo and endo) is too much simplified and a more sophisticated data treatment is advised. This will be done in the subsequent paper.[27]

## Conclusion

Two-dimensional homonuclear NMR spectroscopy can be particularly useful for the analysis of complicated spin systems. The 2-D-*J*-resolved projection spectrum delivers excellent starting parameters for the chemical shifts. The cross sections assist in sorting out overlapping multiplets and provide starting values for coupling constants. Long-range couplings can be readily recognized and assigned via the SECSY spectrum. Finally, stereochemical assignments are often assisted by the 2-D NOE data. A complete spin system analysis yields considerable information concerning solution conformation of the peptide backbone and the proline rings.[27]

## Experimental Section

*cyclo*-(L-$Pro_2$-D-Pro) was synthesized following the procedure of Rothe et al.[28] The synthesis of the derivative deuterated in the $\alpha$ position of $Pro^3$ was performed with racemic $\alpha$-deuterioproline[29] via its *t*-Boc derivative. The linear precursor Boc-($\alpha$-$^2$H)-D,L-Pro-L-$Pro_2$-OTcp was prepared by stepwise C-terminal coupling with H-L-Pro-$OCH_3$ and H-L-Pro-OTcp, and cyclization was performed in the usual manner.[28] The mixture of the two diastereomeric monodeuterated cyclotripeptides *cyclo*-(L-$Pro_2$-($\alpha$-$^2$H)-L-Pro) (**2d**) and *cyclo*-(L-$Pro_2$-($\alpha$-$^2$H)-D-Pro) (**1d**) was purified via chromatography on Sephadex LH 20 (eluant: DMF) and separated over silica gel (eluant: $CHCl_3$/MeOH 9:1): (**2d**) $R_f$ 0.43, (**1d**) $R_f$ 0.51. The 270-MHz $^1H$ NMR spectrum shows the disappearance of the $\alpha$-proton doublet previously assigned to $Pro^3$.

The $^1H$ NMR spectra were recorded with Bruker WH 270 and WM 500 spectrometers at 303 K with sample concentrations of 5–25 mg/mL and $Me_4Si$ as internal standard. For spin simulations one-dimensional spectra were required with a maximum in digital resolution and signal to noise. For the 500-MHz spectra the following parameters were used:

| | in $CD_2Cl_2$ | in $CDCl_3$/$C_6D_6$ (1:8) |
|---|---|---|
| spectral width (Hz) | 2404 | 2703 |
| data size | 64K | 64K |
| acquisition time (s) | 13,6 | 12,1 |
| number of transients | 512 | 296 |

Prior to Fourier transformation the FID was resolution enhanced via the Lorentz-to-Gauss line-shape transformation of Ernst.[30] Parameters were chosen by trial and error to give the best compromise for signal to noise, and resolution of long-range couplings. The PANIC program[14] was used for simulations on the Bruker ASPECT 2000 computer with 80K memory, so that the proline spectral region could be examined with 24K data points each in the experimental and calculated spectra. The digital resolution was the main factor limiting the precision of the iterative analysis (0.073 Hz/point in $CD_2Cl_2$, 0.082 Hz/point in $CDCl_3/C_6D_6$). The $Pro^1$ spin system could be fully assigned and iterated in $CD_2Cl_2$ solvent. The $Pro^3$ system could be iterated for the $CDCl_3/C_6D_6$ mixture. The $Pro^2$ system could not be adequately assigned for iteration of the complete seven-spin system. The results presented for $Pro^2$ represent the "best" fit judged by visual comparison and iteration of selected multiplets.

The two-dimensional $^1H$ NMR experiments at 500 MHz were performed on the sample in $CDCl_3/C_6D_6$ (1:8) solvent. Details for each experiment are described below. Quadrature detection with four-phase transmitter cycling was used exclusively, and the 90° pulse length was 9.7 $\mu$s.

**2-D *J*-Resolved Spectrum.** The pulse sequence 90°-$t_1$/2-180°-$t_1$/2-FID($t_2$) was used. The number of sampled data points was 64 in $t_1$ and 8K in $t_2$. The data were multiplied in $t_2$ with a sine-bell function. A $\pi$/6-shifted sine-bell function and zero-filling to 128 data points was used in the $t_1$ dimension. The spectral width in $\omega_1$ was ±40.7 Hz, in $\omega_2$ 2600 Hz. Eight transients for each $t_1$ increment were collected. The total measuring time was 1.5 h. The 128 × 8K transform required ca. 50 min and the conventional 45° tilt and projection were performed.

**SECSY Spectrum.** The pulse sequence 90°-$t_1$/2-90°-$t_1$/2-FID($t_2$) was used; 512 increments in $t_1$ and 2048 data points in $t_2$ were recorded. The FIDs were multiplied in both dimensions with a sine-bell function and zero-filled before FT. The spectral width was ±900 Hz in $\omega_1$ and 2600 Hz in $\omega_2$. Phase cycling for quadrature detection in both dimensions

(26) Kessler, H.; Friedrich, A.; Krack, G.; Hull, W. E. In ref 24a, p 335.
(27) de Leeuw, F. A. A. M., Altona, C.; Kessler, H.; Bermel, W.; Friedrich, A.; Krack, G.; Hull, W. E. *J. Am. Chem. Soc.*, submitted for publication.
(28) Rothe, M.; Mästle, W. "Peptides 1978", Siemion, J. Z., Kupryszewski, G., Eds.; University Press: Wroclaw, 1979; p 179.
(29) Upson, D. A.; Hruby, V. *J. Org. Chem.* **1977**, *42*, 2329.
(30) Ernst, R. R. *Adv. Magn. Reson.* **1966**, *2*, 1.
(31) **Note Added In Proof**: A 2-D $^1H$-$^{13}C$ shift correlation proves unequivocally this assignment.

was used; 16 transients were taken for each $t_1$ increment, and the total measuring time was 8.6 h. The 1K × 4K transform required ca. 3 h.

**NOE 2-D Spectrum.** The pulse sequence $90°-t_1/2-90°-\tau_m-90°-t_1/2-\mathrm{FID}(t_2)$ was used with a randomized[20] mixing time of 1 s. The data were treated as described for the SECSY spectrum; 16 transients were taken for each $t_1$ increment, and the total measuring time was 11.5 h. The 1K × 4K transform required ca. 3 h. In this experiment with three pulses a 16-phase cycle is not sufficient to eliminate quadrature image signals, which appear on a line of slope $^1/_2$ intersecting the $\omega_1 = 0$ axis at $\omega_2 = 0$ (the position of the RF carrier for quadrature detection). The line of image peaks is denoted by arrows in Figure 8.

**Acknowledgment.** We thank the Deutsche Forschungsgemeinschaft and the Fonds der Chemischen Industrie for financial support.

**Registry No.** **1d**, 83174-89-4; **2d**, 83199-50-2; BOC-($\alpha$-$^2$H)-D,L-Pro-L-Pro$_2$-OTcp, 83174-88-3; *cyclo*-(L-Pro$_2$-D-Pro), 70493-40-2.

# Optical vs. Thermodynamic Basicities: Probe $Pb^{2+}$ Ion Spectra in Thermodynamically Characterized Molten Chloroaluminate Solutions

**C. A. Angell* and P. D. Bennett[1]**

*Contribution from the Department of Chemistry, Purdue University, West Lafayette, Indiana 47907.* *Received April 30, 1982*

**Abstract:** The energy of the outer-shell $^3P_1 \leftarrow {}^1S_0$ transition of $Pb^{2+}$ doped into various binary chloroaluminate solutions has been studied in an attempt to gain insight into the changes in electronic states of anions in a binary chloride solution state as the composition is changed through a region of abrupt thermodynamic changes (equivalence point). Sudden shifts in the band maximum of as much as 3000 $cm^{-1}$ are observed to occur at the stoichiometry of $AlCl_4^-$, the range over which the change occurs closely matching the 0.5 mol % wide region of rapid chloride activity change observed in earlier measurements. In the case of the low-melting system $AlCl_3$ + ethylammonium chloride, spectra were taken at 0.05 mol % intervals at 90 °C and it was noted that the entire energy shift occurred across a 0.2 mol % gap in which the $Pb^{2+}$ was quantitatively rejected from solution (presumably as $PbCl_2$ although $Pb(AlCl_4)_2$ has not been excluded). In this case a second composition region of spectral shift was found that corresponds with one in which NMR studies in a related system also indicate a second acid-base process. The correlation with thermodynamically determined basicity changes in these systems is good enough to justify the use of $Pb^{2+}$ as a basicity indicator and to lend credence to the optical basicity scale proposed on the basis of the nephelauxetic effect for $d^{10}s^2$ cations in acid media. However, measurements to be reported separately on the isoelectronic $Tl^+$ and $Bi^{3+}$ spectra in the same systems show that caution is necessary. An ion in this series will only be an effective and reliable indicator for basicity changes if, as for aqueous acid-base indicators, it is approximately midway in basicity between the acidic and basic species being reacted.

## Introduction

The basic chemical study described in this paper has been motivated by a need to resolve a problem impeding the development of an understanding of physical processes in technically important inorganic glasses. It has been known for a long time that structural features of ionic liquids and glasses such as the coordination number of a transition-metal ion, and chemical features such as oxidation states, are strongly dependent on what is loosely referred to as the "basicity" of the glass.[2] However, it has only recently been realized that important dynamic properties such as the electrical conductivity are also closely related to the same quantity.[3] Given the current surge of interest in glasses as fast ion solid electrolytes, it is now more important than ever that means of quantifying the concepts involved in the terms "basicity" and "oxide ion activity", and in particular of making comparisons between systems of quite different composition, be developed.

For individual liquid binary systems, the "basicity" can be defined quite precisely in terms of the thermodynamic activity of the more basic component as determined by, e.g., electrochemical or conventional vapor pressure methods. Although such measurements are not simple in hot corrosive liquids, they have been performed in limited composition ranges in such fundamental systems as $Na_2O + SiO_2$. In this system $a_{Na_2O}$ ($=a_\pm^2$) has been widely studied in both liquid and vitreous states. However, if a comparison of physical or chemical behavior in two different binary systems, e.g., $Na_2O + SiO_2$ and $Li_2O + GeO_2$, is desired, thermodynamics is limited in its ability to help, even though it seems clear that the differences in behavior observed have much to do with the quantity conceptualized, but not quantified, as "basicity" or "oxide ion activity". The best that can be done is to probe each system with a test species whose activity would be measured.

Another problem is raised on passing to the glassy state, in which thermodynamic equilibrium is not maintained. Due to the mobility of certain components of the glass structure, electrochemical measurements can still be performed and variations of chemical potential with composition can be measured,[3] but their precise relation to the corresponding liquid-state properties is clouded, particularly when the glass transition temperature $T_g$ is highly composition dependent.

In view of these problems it is of interest to develop nonthermodynamic probes of the chemical state of the liquid or glass, probes that are sensitive to the states of chemical binding or polarization of the ionic or quasi-ionic components of the system, which, after all, determine the thermodynamic activities under discussion. Such probes will be most helpful if their behavior can be shown to exhibit the same response to composition changes as does the thermodynamic basicity or some suitable function of it.

(1) Present address: Standard Oil of Ohio, Cleveland, OH 44115.

(2) Detailed reviews and analysis of this problem area are given in: (a) J. Wong and C. A. Angell, "Glass: Structure by Spectroscopy", Marcel Dekker, New York, 1976; (b) C. A. Angell in "Spectroscopic and Electrochemical Characterization of Solute Species in Non-Aqueous Solutions", G. Mamantov, Ed., Plenum Press, New York, 1977, p 273.

(3) (a) D. Ravaine and J. L. Souquet, *Phys. Chem. Glasses*, **18**, 27 (1977); (b) D. Ravaine, *J. Non-Cryst. Solids*, **38-39**, 353 (1980); (c) J. L. Souquet, *Solid State Ionics*, in press.

0002-7863/82/1504-6304$01.25/0 